Biophysical Letter

Improving Survival of Disassociated Human Embryonic Stem Cells by Mechanical Stimulation Using Acoustic Tweezing Cytometry

Di Chen,[1] Yubing Sun,[2] Cheri X. Deng,[1,*] and Jianping Fu[2,*]
[1]Department of Biomedical Engineering and [2]Department of Mechanical Engineering, University of Michigan, Ann Arbor, Michigan

ABSTRACT Dissociation-induced apoptosis of human embryonic stem cells (hESCs) hampers their large-scale culture. Herein we leveraged the mechanosensitivity of hESCs and employed, to our knowledge, a novel technique, acoustic tweezing cytometry (ATC), for subcellular mechanical stimulation of disassociated single hESCs to improve their survival. By acoustically actuating integrin-bound microbubbles (MBs) to live cells, ATC increased the survival rate and cloning efficiency of hESCs by threefold. A positive correlation was observed between the increased hESC survival rate and total accumulative displacement of integrin-anchored MBs during ATC stimulation. ATC may serve as a promising biocompatible tool to improve hESC culture.

Received for publication 3 September 2014 and in final form 28 January 2015.

*Correspondence: cxdeng@umich.edu or jpfu@umich.edu

Di Chen and Yubing Sun contributed equally to this work.

Human embryonic stem cells (hESCs) hold indefinite self-renewing capacity in vitro. However, their large-scale maintenance and expansion are significantly hindered by dissociation-induced apoptosis, leading to extremely low single-cell cloning efficiency (<1%). Although the discovery that inhibition of Rho-associated kinase (ROCK) can significantly improve survival of dissociated hESCs may offer a solution (1), long-term effects of treatments of hESCs with ROCK inhibitors are unclear, and such inhibitors have been associated with aneuploidy, which is implicated in cell transformation. In addition, because myosin II activity, a downstream effector of ROCK, is involved in formation of cleavage furrow and cytokinesis, long-term exposure to ROCK inhibitors can inhibit cell division to negatively impact hESC cloning efficiency (2,3). Consequently, passaging hESCs by mechanically cutting large colonies into small clumps is still a routine practice used in stem cell laboratories.

Recently, we and others have demonstrated that hESCs are intrinsically mechanosensitive and that their self-renewal and differentiation are influenced by biophysical signals including mechanical forces and matrix rigidity (4–6). Here we leveraged a newly developed technique, acoustic tweezing cytometry (ATC), to explore whether mechanobiology might be exploited for improving hESC culture. We specifically examined whether subcellular mechanical forces exerted by ATC might improve survival of disassociated single hESCs (7). In ATC, ultrasound pulses are utilized to acoustically excite functionalized lipid-encapsulated microbubbles (MBs) targeted to cell-surface integrin receptors to apply subcellular forces through MB-integrin-actin cytoskeleton linkage (Fig. 1 *a*) (7) and cell membrane (8).

For ATC stimulation of hESCs, disassociated single hESCs were first seeded on tissue culture plates at a density of 10,000 cells cm^{-2} for 1 h followed by 10-min incubation with MBs (3×10^7 mL^{-1}) functionalized with Arg-Gly-Asp (RGD) peptides (RGD-MBs) using avidin-biotin conjugation chemistry to allow specific integrin binding. Ultrasound pulses (center frequency 10 MHz, pulse duration 50 ms, pulse repetition frequency 10 Hz, acoustic pressure 0.08 MPa) were then applied to hESCs bound with RGD-MBs for 30 s every hour for 4 h, consecutively (Fig. 1, *b* and *c*, and see the Supporting Material).

Live cell imaging was performed using a synchronized high-speed camera to monitor dynamic changes of cell morphology and activities of MBs during and after ATC applications (see Methods in the Supporting Material; and see Fig. 1 *d*). MBs exhibited robust responses to ultrasound pulses, including displacements due to the acoustic radiation forces (9) acting on MBs (7) (see Movie S1). As expected, for negative controls without MBs and without ultrasound (US) treatments (−US/−MB), most hESCs upon cell seeding exhibited marked changes in cell morphology that included cell body contraction and membrane blebbing before undergoing apoptosis within 24 h after disassociation, resulting in a limited survival rate of 16.8 ± 3.1% ($n = 5$) (Fig. 1 *e*). Notably, for hESCs attached with RGD-MBs, ATC treatments elicited spreading of the originally rounded hESCs and their adherence to tissue culture

Editor: Christopher Yip.
© 2015 by the Biophysical Society
http://dx.doi.org/10.1016/j.bpj.2015.01.033

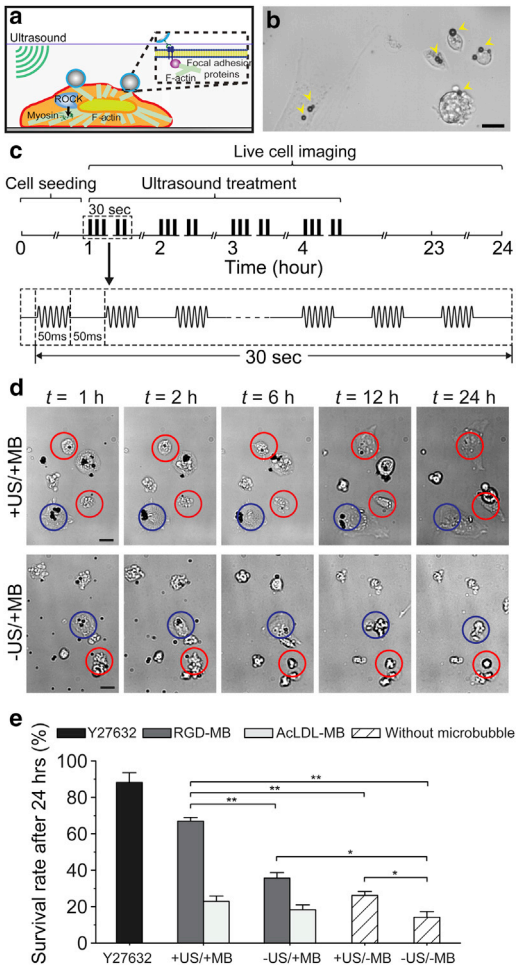

FIGURE 1 (*a*) ATC stimulation by acoustic excitation of MBs attached to cells. (*b*) Bright-field image showing hESCs attached with MBs. Scale bar, 20 μm. (*c*) Illustration of ultrasound protocol. (*d*) Live cell imaging showing hESCs exposed to ATC. Rounded hESCs (*red circles*) with spread hESCs (*blue circles*). Scale bar, 10 μm. (*e*) Survival rate of hESCs exposed to ATC treatments with RGD-MBs, AcLDL-MBs, and without MB ($n = 5$, number of cells in each experiment > 200). Error bars, mean $\pm$ SE; $^{**}p < 0.01$, $^{*}p < 0.05$, Student's *t*-test. To see this figure in color, go online.

plates. As a result, 67.0 $\pm$ 2.0% ($n = 5$) of such cells survived within 24 h after disassociation (+US/+MB; Fig. 1, *d* and *e*; Movie S2). hESCs that have already spread before ATC treatments also survived for at least 24 h regardless of the presence of MBs or US treatment (Fig. 1 *d*), suggesting that cell spreading and adhesion might be critical for promoting hESC survival. Interestingly, ultrasound application alone (+US/−MB) or the presence of RGD-MBs alone (−US/+MB) had marginal but significant effect in enhancing hESC survival, resulting in a survival rate of 28.6 $\pm$ 2.2% ($n = 5$) for hESCs without MBs but treated with ultrasound (+US/−MB) (Fig. 1 *e*), and 35.7 $\pm$ 3.0% ($n = 5$) for hESCs with RGD-MBs but without ultrasound treatment (−US/+MB; Fig. 1 *e*). These results suggest that binding of RGD-MBs may trigger adhesion signaling and promote hESC survival.

To further investigate the role of integrin-mediated adhesion in hESC survival, we conducted experiments to apply ATC treatments to hESCs conjugated with MBs coated with acetylated low-density lipoprotein (AcLDL; AcLDL-MBs), a ligand for transmembrane metabolic receptors that does not bind integrins. Under the same ATC treatments, the survival rate of hESCs with AcLDL-MBs was unchanged compared to cells without MBs (−US/−MB and +US/−MB; Fig. 1 *e*), even though AcLDL-MBs exhibited significantly greater displacements than RGD-MBs (data not shown). These data suggested that integrin-mediated adhesion was required for improved hESC survival by acoustic actuation of integrin-anchored RGD-MBs.

To ascertain details of acoustic actuation of integrin-anchored RGD-MBs on hESCs, we divided originally rounded single hESCs into different subgroups based on the initial number of RGD-MBs attached to each cell (Fig. 2 *a*). We examined hESC survival rate and the corresponding MB displacements for each subgroup. hESCs with two or more RGD-MBs per cell exhibited a significantly greater survival rate than cells with no or only one RGD-MB under ATC treatments (Fig. 2 *b*). The total accumulative RGD-MB displacement per cell for hESCs with two to four RGD-MBs was also significantly greater than that for hESCs with only one RGD-MB per cell (Fig. 2 *c*). It should be noted that the heightened total accumulative displacement of RGD-MBs was not only due to the greater number of RGD-MBs per cell, but also from the secondary acoustic radiation forces between MBs (9), which could efficiently displace MBs toward each other (Movie S3). For

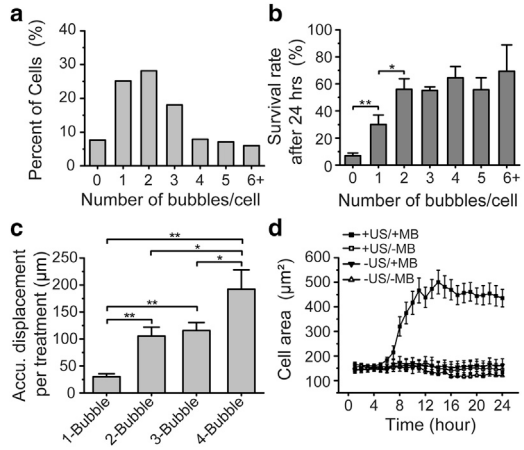

FIGURE 2 (*a*) Distribution of MBs per cell (five independent experiments, $n > 200$ cells for each). (*b*) Survival rate of hESCs with different initial numbers of RGD-MBs/cell; $n > 200$ cells for each experiment, $n > 20$ cells for each subgroup with different number of MBs per cell. Error bars, mean $\pm$ SE; $^{**}p < 0.01$, $^{*}p < 0.05$, Student's *t*-test. (*c*) Accumulative MB displacement per ATC treatment. Error bars, mean $\pm$ SE; $^{**}p < 0.01$, $^{*}p < 0.05$, Student's *t*-test. (*d*) Change of cell area for different subgroups.

hESCs with three RGD-MBs per cell, the total accumulative MB displacement was similar to two-bubble cases (Fig. 2 *c*), because one of the three MBs often exhibited a minimal movement (Movie S4) with balance of forces in the presence of multiple MBs and mutual interactions among them. Four-MB cases could be considered as a combination of one-, two-, and/or three-MB cases with variations in the patterns of individual MB movements depending on their relative locations with each other on the cells (Fig. 2 *c*; Movie S5). In addition, initially rounded hESCs bound with RGD-MBs and treated with ATC stimulations (+US/+MB) initiated their spreading ~5 h after cell seeding and became fully spread by 12 h (Fig. 2 *d*), significantly slower than conventional cell-spreading processes (10). Areas of hESCs without MBs (+US/−MB) or with MBs but without ultrasound treatments (−US/+MB) remained unchanged during the first 24 hours after cell seeding (Fig. 2 *d*), corresponding to low survival rates for these groups.

To evaluate possible long-term effects of ATC treatment, we conducted an alkaline phosphatase (ALP) assay to determine hESC cloning efficiency. Consistent with improved initial survival rate, cloning efficiency of ATC-treated hESCs increased approximately threefold compared to untreated −US/−MB controls (Fig. 3, *a* and *b*), suggesting that the effect of ATC was mainly the improvement of initial survival of disassociated hESCs rather than cell proliferation or migration (11,12). ATC treatments did not adversely impact hESC stemness marker expression, as shown by positive immunostaining of pluripotency markers Oct4, Sox2, and E-cadherin 7 days after ATC treatments (Fig. 3 *c*).

Collectively, our data indicate that ATC stimulations improve the clonogenicity of disassociated hESCs by increasing their initial survival rate. While the molecular mechanism underlying such mechanosensitive behavior of hESCs requires further study, our results suggest that integrin-mediated adhesion formation and strengthening by ATC stimulations may facilitate spreading of disassociated hESCs, which in turn rescues the cells from hyperactivated actomyosin activities triggering downstream caspase-mediated apoptotic signaling pathways.

Compared to established methods for applying subcellular forces using solid microbeads (i.e., optical and magnetic tweezers), ATC utilizes MBs that do not exhibit cellular internalization and can be easily removed from hESCs without leaving behind exogenous materials, providing a promising biocompatible platform for large-scale hESC culture.

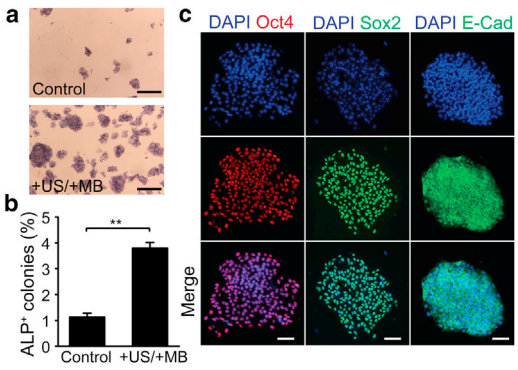

FIGURE 3 (*a*) ALP assay for dissociated hESCs with or without ATC treatments as indicated. Scale bar, 1 mm. (*b*) Relative ratio of ALP+ colonies to the number of hESCs initially seeded. (*c*) Immunostaining with anti-Oct4, anti-Sox2, and anti-E-cadherin antibodies for hESC colonies 7 days after ATC treatments. Scale bar, 100 μm. To see this figure in color, go online.

SUPPORTING MATERIAL

Supporting Methods, Supporting Discussion, and five movies are available at http://www.biophysj.org/biophysj/supplemental/S0006-3495(15)00128-9.

ACKNOWLEDGMENTS

This work is supported in part by the National Science Foundation (grants No. CMMI 1129611 and No. CBET 1149401), the National Institutes of Health (grants No. R21 HL114011 and No. R21 EB017078), and the American Heart Association (grant No. 12SDG12180025).

REFERENCES

1. Watanabe, K., M. Ueno, …, Y. Sasai. 2007. A ROCK inhibitor permits survival of dissociated human embryonic stem cells. *Nat. Biotechnol.* 25:681–686.
2. Chen, G., Z. Hou, …, J. A. Thomson. 2010. Actin-myosin contractility is responsible for the reduced viability of dissociated human embryonic stem cells. *Cell Stem Cell.* 7:240–248.
3. Ohgushi, M., M. Matsumura, …, Y. Sasai. 2010. Molecular pathway and cell state responsible for dissociation-induced apoptosis in human pluripotent stem cells. *Cell Stem Cell.* 7:225–239.
4. Sun, Y., L. G. Villa-Diaz, …, J. Fu. 2012. Mechanics regulates fate decisions of human embryonic stem cells. *PLoS ONE.* 7:e37178.
5. Keung, A. J., P. Asuri, …, D. V. Schaffer. 2012. Soft microenvironments promote the early neurogenic differentiation but not self-renewal of human pluripotent stem cells. *Integr. Biol. (Camb).* 4:1049–1058.
6. Sun, Y., K. M. Yong, …, J. Fu. 2014. Hippo/YAP-mediated rigidity-dependent motor neuron differentiation of human pluripotent stem cells. *Nat. Mater.* 13:599–604.
7. Fan, Z., Y. Sun, …, J. Fu. 2013. Acoustic tweezing cytometry for live-cell subcellular modulation of intracellular cytoskeleton contractility. *Sci. Rep.* 3:2176.
8. Heureaux, J., D. Chen, …, A. P. Liu. 2014. Activation of a bacterial mechanosensitive channel in mammalian cells by cytoskeletal stress. *Cell. Mol. Bioeng.* 7:1–13.
9. Dayton, P. A., K. E. Morgan, …, K. W. Ferrara. 1997. A preliminary evaluation of the effects of primary and secondary radiation forces on acoustic contrast agents. *IEEE Trans.* 44:1264–1277.
10. Bardsley, W. G., and J. D. Aplin. 1983. Kinetic analysis of cell spreading. I. Theory and modeling of curves. *J. Cell Sci.* 61:365–373.
11. Barbaric, I., V. Biga, …, P. W. Andrews. 2014. Time-lapse analysis of human embryonic stem cells reveals multiple bottlenecks restricting colony formation and their relief upon culture adaptation. *Stem Cell Rep.* 3:142–155.
12. Li, L., B. H. Wang, …, L. Wang. 2010. Individual cell movement, asymmetric colony expansion, rho-associated kinase, and E-cadherin impact the clonogenicity of human embryonic stem cells. *Biophys. J.* 98:2442–2451.

Biophysical Journal

Supporting Material

Improving Survival of Disassociated Human Embryonic Stem Cells by Mechanical Stimulation Using Acoustic Tweezing Cytometry

Di Chen, Yubing Sun, Cheri X. Deng, and Jianping Fu

Supporting Methods

Attachment of targeted microbubbles to cells

The cell-seeded 35-mm glass bottom dish was placed on a 37°C heating stage on an inverted microscope (Eclipse Ti-U; Nikon, Melville, NY). Cells were bound with targeted Arg-Gly-Asp peptide (RGD) coated microbubbles (RGD-MB) or acetylated low density lipoprotein (AcLDL) coated microbubbles (AcLDL-MB). To form RGD-MB, Targesphere™-SA microbubbles (Targeson, San Diego, CA) were mixed with biotinylated RGD molecules (Peptides International, Louisville, KY) for 20 min at room temperature, with a volume ratio of 5:1 between MBs (3×10^9 mL^{-1}) and RGD (2 mg mL^{-1}). As a negative control, AcLDL-MBs, without mechanical linkages to the intracellular actin cytoskeleton (CSK), were obtained by mixing MBs with AcLDL (Invitrogen, Carlsbad, CA) for 24 hr at 4°C with a volume ratio of 5:1 between MBs (3×10^9 mL^{-1}) and AcLDL (2.5 mg mL^{-1}). To conjugate MBs to disassociated hESCs, the culture medium from the cell-seeded dish was removed followed by immediate addition of 20 μL of the diluted (1:100 by volume in PBS) RGD-MB or AcLDL-MB solution. The petri dish was then flipped over for 10 min, so that attached cells on the glass bottom dish faced downward to facilitate attachment of MBs to the cells. The dish was flipped back, and unbound MBs were removed by a gentle wash with culture medium (Fig. 1b).

Cell culture and disassociation

hESC line H1 (WiCell) was cultured on mitotically inactive mouse embryonic fibroblasts (MEFs; GlobalStem) in growth medium with daily medium change. Growth medium contained DMEM/F12 (GIBCO), 20% KnockOut serum replacement (GIBCO), 0.1 mM β-mercaptoethanol (GIBCO), 2 mM glutamax (GIBCO), 1% non-essential amino acids (GIBCO), and 4 ng mL^{-1} human recombinant basic fibroblast growth factor (bFGF; GlobalStem). Cells were rinsed briefly with PBS and treated with TrypLE Select (Invitrogen) for 2 min to release MEFs. Cells were rinsed briefly again with PBS before all cells, including hESCs and remaining MEFs, were collected using a cell scraper (BD Biosciences). To remove contaminant MEFs, all cells were transferred onto a 60-mm tissue culture dish (BD Biosciences) coated with gelatin (Sigma) and incubated for 45 min. MEFs would attach to the dish while hESCs were still in the supernatant.

Single hESCs were seeded on vitronectin coated tissue culture plates immediately after disassociation and after 1 hr, MBs were added to bind the cells. Live cell imaging was then performed to monitor dynamics of morphology changes of hESCs.

Ultrasound system and generation of ultrasound pulses

A 10 MHz focused transducer (Olympus, Waltham, MA, USA), positioned at an angle of 45° was used for ATC experiments. The ultrasound (US) pulses applied in this study had fixed pulse duration (PD) of 50 ms, pulse repetition frequency (PRF) of 10Hz, total application time of 30 s, and acoustic pressure of 0.08 MPa. The transducer was driven by a waveform generator (Agilent Technologies 33250A, Palo Alto, CA) and a 75 W power amplifier (Amplifier Research 75A250, Souderton, PA). By applying US pulses, MBs conjugated to individual cells underwent a cyclic movement and exerted subcellular mechanical forces to live single cells.

Quantification of cell survival rate and cell area

A live cell imaging system was utilized to monitor dynamics of morphology changes of hESCs from 1 hour till 24 hour after the disassociated cells are seeded. The survival rate after 24 hours (Fig. 1e) is defined as the number of cells survived at t = 24 h divided by the total number of cells at t = 1h. Similarly, survival rate in Fig. 2b is defined as the corresponding number of survived cells at t = 24 h that were initially rounded divided by the total number of rounded cells at t = 1h with different number of microbubbles attached. Cells of interest were selected from the recorded image sequences using Image J (U. S. National Institutes of Health) and the cell area were estimated by tracing the boundary of the cell.

Characterization of ultrasound-driven microbubble kinetics

A high-speed camera (Photron FASTCAM SA1, San Diego, CA) was used for observation of microbubble activities during the 30 s of ultrasound application at a frame rate of 500 frames s^{-1}. Pixel intensity and its spatial gradient of the acquired images were used to track microbubbles using a customized algorithm refined from built-in circle tracking algorithms in Matlab (Mathworks). The displacement of a microbubble was

obtained from these images as a functional of time from its original location. The accumulative bubble displacement (Fig. 2c) was estimated as the summation of the bubble displacements sustained during all of the ultrasound pulses applied in the 30s treatment.

Supporting Discussion

Adhesion-mediated survival of hESCs

Our results indicated that integrin-mediated adhesion signaling might be important for promoting survival of single hESCs. Supporting this view, it has been nicely demonstrated that dissociation induced hESC apoptosis is not due to a loss of cell-ECM adhesion (1). Furthermore, removing Y27632 after cell spreading for 6-12 hrs does not affect survival of single hESCs (1). Integrin-mediated adhesion signaling trigged by binding of RGD-MB but not AcLDL-MB (Fig. 1e) may very likely suppress apoptosis signaling in hESCs. In addition, ATC stimulation may further strengthen integrin-mediated adhesion formation and thus further reduce apoptosis of single hESCs. As shown in Fig. 2d, integrin-mediated adhesion formation and strengthening by ATC stimulations further facilitated cell spreading of disassociated hESCs, which in turn increased cell adhesion to rescue the cells from hyper-activated actomyosin activities triggering downstream caspase-mediated apoptotic signaling pathways.

Supporting Movies

Movie S1. High speed recording of one-bubble case during ATC (first 3 s, 500 frame/s). Scale bar, 10 μm.

Movie S2. Time lapse live-cell images of hESCs for 24 hrs. Scale bar, 10 μm.

Movie S3. High speed recording of two-bubble case during ATC (first 3 s as shown, 500 frame/s). Scale bar, 10 μm.

Movie S4. High speed recording of three-bubble case during ATC (first 3 s as shown, 500 frame/s). Scale bar, 10 μm.

Movie S5. High speed recording of four-bubble case during ATC (first 3 s as shown, 500 frame/s). Scale bar, 10 μm.

Supporting References

1. Ohgushi, M., M. Matsumura, M. Eiraku, K. Murakami, T. Aramaki, A. Nishiyama, K. Muguruma, T. Nakano, H. Suga, M. Ueno, T. Ishizaki, H. Suemori, S. Narumiya, H. Niwa, and Y. Sasai. 2010. Molecular Pathway and Cell State Responsible for Dissociation-Induced Apoptosis in Human Pluripotent Stem Cells. Cell Stem Cell 7:225-239.